PFG 2014 / 4, 0253 – 0263
Stuttgart, August 2014

Article

MACS-TumbleCam – A Novel Approach for Aerial Oblique Imaging

Jörg Brauchle, Wolfgang Rüther-Kindel & Ralf Berger, Berlin

Keywords: oblique camera, aerial imaging, UAV, digital terrain modelling, modular payload concept, MACS-TumbleCam, 3D-model

Summary: The ATISS measurement drone, developed at the University of Applied Sciences Wildau, is an electrical powered autonomous motor glider with a maximum take-off weight of 25 kg including a payload capacity of up to 10 kg. Two engines enable ultra short take-off procedures and the motor glider design results in a 1 h endurance. The concept of ATISS is based on the idea to strictly separate between aircraft and payload functions, which makes it a very flexible research platform for miscellaneous applications.
In a project together with German Aerospace Center (DLR) this carrier was used for demonstrating a novel approach in high-resolution digital terrain modelling.
A lightweight, 3D-capable photogrammetric camera called MACS-TumbleCam was developed at the DLR Berlin especially for the ATISS payload concept. The unique feature of this camera system is the special combination of two synchronized digital cameras with an adjustable relative alignment. One camera head is oriented in a fixed nadir position while the other one can be driven to variable oblique orientations by a robotic actuator. Thus it is possible to take images from very different view directions for almost every object on the ground. Due to a parametric boresight calibration a low-cost inertial orientation system can be used.
The evaluation of the first test flights shows features of the system, i.e. derived high-precision 3D-models of urban structures with 3 cm ground pixel resolution and high-resolution façade textures.

Zusammenfassung: *MACS-TumbleCam – ein neues Verfahren für Schrägluftbilder.* ATISS, eine an der Technischen Hochschule Wildau (FH) entwickelte Messdrohne, ist ein elektrisch angetriebener autonomer Motorgleiter mit einem maximalen Abfluggewicht von 25 kg bei einer Nutzlastkapazität von bis zu 10 kg. Zwei Motoren ermöglichen sehr kurze Startvorgänge und eine Flugzeit von etwa einer Stunde. Das Systemdesign von ATISS basiert auf einer strikten Trennung von Nutzlast- und Flugzeug-Funktionen, was den Träger zu einer flexiblen Forschungsplattform für unterschiedliche Anwendungen macht.
In einem gemeinsamen Projekt mit dem Deutschen Zentrum für Luft- und Raumfahrt (DLR) konnte mit diesem Träger ein neuartiges Konzept zur hochauflösenden luftgestützten Geländemodellierung demonstriert werden.
Dazu wurde vom DLR ein sehr kompaktes 3D-fähiges Luftbildkamera-System (MACS-TumbleCam) entwickelt. Dieses Konzept kombiniert zwei synchronisierte Kameras mit einer Aktuatorik zur schnellen Veränderung der Relativlage. Dabei schaut ein Kamerakopf senkrecht (nadir), der zweite ist dem gegenüber mit einem variablen Sichtwinkel (oblique) ausgerichtet. Dies ermöglicht die weitgehend vollständige hochgenaue Abbildung von Objekten aus unterschiedlichen Perspektiven. Eine parametrische Boresight-Kalibrierung ermöglicht die Nutzung eines low-cost Orientierungssystems.
Die Auswertung erster Testflüge zeigt die Fähigkeiten des Gesamtsystems. So konnten aus den Daten des Kamerasystems hochgenaue 3D-Modelle urbaner Strukturen mit 3 cm Bodenpixelauflösung inklusive hochauflösender Fassadentexturen gewonnen werden.

www.schweizerbart.de
DOI: 10.1127/1432-8364/2014/0200
1432-8364/14/0200 $ 3.00

1 Introduction

Aerial imaging from small unmanned aircrafts (UAVs) has become an emergent topic in recent years (Eisenbeiss 2009). The rise was mainly caused by the availability of low-priced but mature aerial vehicles. Applications range from surveillance and reconnaissance to environmental or agricultural monitoring as well as mapping and photogrammetry (Zhang & Kovacs 2012, Heinze et al. 2010, Remondino 2011).

Apart from military systems, mostly small multicopter or fixed wing aircraft are used, with a maximum take-off weight less than 5 kg. Since there are no photogrammetric camera systems available that can be carried by such limited aircraft, the usual approach is to operate commercial consumer cameras together with a low-cost GPS receiver (Cramer et al. 2013, Neitzel & Klonowski 2011, Küng et al. 2011a).

Evaluation of such data is often done based on structure-from-motion approaches. While this gives fast and visually appealing results, positional accuracy of the data is difficult to determine.

The first UAV (unmanned aerial vehicle) project at the University of Applied Sciences Wildau started in 2006. It was called SMAP (smart aerial photogrammetry system) and was based on a market-available fixed wing model aircraft. The aim was to demonstrate that small UAV are capable of carrying a calibrated aerial camera to produce aerial images of a quality comparable to man operated systems. A Trimble AIC camera system was integrated in the fuselage together with a navigation system, an on-board computer and a telemetry system.

This project was successfully completed. However, it showed that neither the carrier aircraft nor the camera system was ideal for this kind of mission. The main disadvantages were vibrations from the piston engine, the limited access to the camera system in the narrow fuselage and the total weight of the system. As a consequence it was decided to develop a new carrier aircraft especially designed for multi role measurement tasks.

2 The ATISS UAV

Based on the experiences of this first project the system design of UAV ATISS (Autonomous Flying Testbed for Integrated Sensor Systems) was started in 2007. The key requirements for this new aircraft were

1. separation of payload and carrier functions,
2. electrical propulsion system,
3. easy access payload concept,
4. motor glider design for low energy consumption,
5. low approach speed of 10 m/s,
6. maximum take-off weight of 25 kg, and
7. payload up to 10 kg.
8. Configuration and construction were carried out as a bachelor thesis (Danders 2007), see Fig. 1.

The final production took place in the aeronautics research lab of the working group, with the first flight performed in summer 2009, see Fig. 2.

The maximum take-off weight of 25 kg was chosen due to legal restrictions in Germany (Seiler 2013), but it can be extended if required. The actual payload capacity of 10 kg gives enough flexibility for a large choice of equipment. Speed range is from 10 m/s to 40 m/s, typical operation speed is 18 m/s for

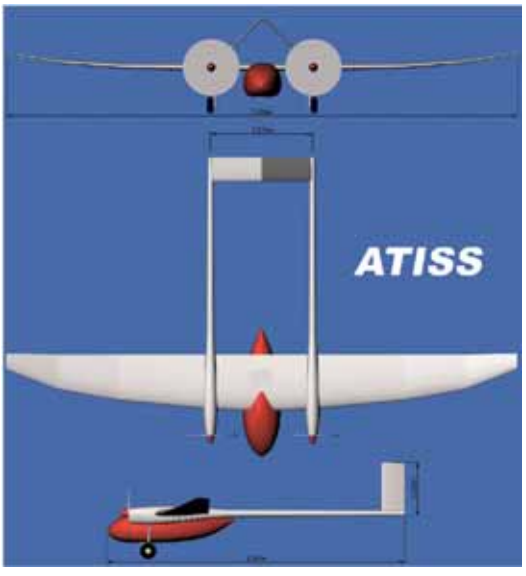

Fig. 1: ATISS (autonomous flying testbed for integrated sensor systems) design.

Fig. 2: ATISS UAV first flight.

Fig. 3: Payload concept CONTAIN.

an endurance of approximately 1 h, which can be increased by reducing the payload weight.

The modular and easy access payload concept CONTAIN (concept for autonomous operating aerial sensor payloads) is shown in Fig. 3. The rack system offers a payload compartment of 220 × 220 × 400 mm³ volume. The rail system enables easy and fast access to the payload.

The first project for the newly developed aircraft was called SALSA (smart airborne laser scanner) and aimed to integrate a laser scanner for digital terrain modelling. It was clear that it would be difficult to combine a laser scanner with an aerial camera within the ATISS payload limit of 10 kg. After technical discussions with the German Aerospace Center, the technical concept was completely revised in favour of an innovative multihead camera system instead of a laser scanner, combined with a high-end direct georeferencing device. This new payload idea has considerable advantages regarding costs, weight, ground resolution and accuracy.

3 Aerial Camera MACS-TumbleCam

Remote sensing on unmanned platforms offers enormous demands for photogrammetric cameras. However, ad hoc developed systems are practically lacking. The requirements for sophisticated sensor systems are challenging, particularly with respect to dimensions and weight. The pursuit of higher ground sampling distances in the centimetre range requires the carrier to be closer to the target, utilizing smaller electrically powered carriers. One or more circular or linear flight paths over a distinctive object are often shown, followed by computer-based modelling of this object (Küng et al. 2011b, Li & Li 2011, Wenzel et al. 2013). Flight times of 15 min to 30 min are common until the need for touch-down.

The Institute of Optical Sensor Systems at the DLR developed the "Modular Airborne Camera Systems (MACS)", which are a family of highly specialized aerial cameras with many practical applications (Lehmann et al. 2011). When deploying this concept, advanced requirements of the mission can be fulfilled.

With MACS-TumbleCam a new method of acquiring oblique images is realized. Thus, the target area of airborne surveys can be increased considerably. Practical demonstration was carried out during several test flights with the ATISS UAV in 2012. High precision geoinformation can be derived using images of this lightweight measurement camera system, e.g. fully texturized 3D-models.

3.1 *Requirements*

As described in chapter 2, the concept of ATISS is based on a strict separation of carrier and payload functions. Thus, a self-sustaining 3D-capable aerial camera system was developed. ATISS provides payload dimensions of 220 × 220 × 400 mm³ (W × H × L) and a weight of up to 10 kg. All peripherals such as power supply, GNSS system with support by an inertial measurement unit (IMU) and computational devices had to be integrated into the pod. Actual weight and dimensions of the camera system are listed in Tab. 1. The main objective was to acquire high-grade images

Tab. 1: Setup MACS-TumbleCam.

Imaging sensors	RGB CCD, 3296 x 2472 pixels, 5.5 µm pixel pitch
Camera quantity	2, one nadir and one oblique
Ground sampling distance	~2 cm @ 100 m height (above ground)
Radiometric resolution	12 bit raw image
Focal length	35 mm each camera
Image rate	5 Hz maximum
Arrangement	1x nadir + 1x oblique with tilt angle of ~30 deg and arbitrary rotation
Actuator tumbling camera	Rotational stage, 34 µrad encoder resolution
Direct georeferencing	Post-processed L1/L2 GNSS + MEMS AHRS
Computer	3.5“ single board, Atom D525, Linux, 2x 256 GB SSD
On-board recording	~40,000 images
Telemetry	868 MHz
Dimensions	400 x 220 x 200 mm^3 (L x W x H)
Weight	<4 kg (<5 kg with LiPo battery)
Power supply	LiPo battery for 1 h operation, or 9 – 36 VDC

to facilitate accurate models of the surveyed area, therefore photogrammetric cameras are used. Good exterior orientation parameters for all images had to be delivered to assist the aerial triangulation (AT) in post-processing. For visualization of realistic façades, views of the target from different directions had to be acquired. Due to the fixed wing flight characteristics of ATISS parallel lines are flown.

3.2 *The Tumbling-Concept*

These requirements imply that conventional methods of taking oblique images could not be adopted. Taking a penta-camera head (5 fixed cameras with 1 nadir and 4 main oblique axes) would lead to too much weight, energy consumption and computer capacities. On the other hand a triple-camera head (3 fixed cameras with 1 nadir and 2 left-right oblique axes) would reduce the ground coverage by approximately 50% at a given flight endurance, because there is the need for additional flight lines to acquire all 4 main oblique perspectives.

A new approach to acquire multiple perspectives using only one camera is given by the tumbling sensor, see Fig. 4: The camera (C) is biaxially gimbal-mounted. It can be arbitrarily deflected from the not gimballed axis (z). This converts the camera into an oblique camera. Fixed by a catch (B), the oblique angle is defined by distances between catch and gimbal origin, (r) and (h). Here a configuration with fixed radius (r) is introduced. If radius (r) was variable, the oblique angle would be variable accordingly. The catch is mounted on a rotary element (A) and describes a circular path which is the only remaining degree of freedom. By rotating (A) the camera is forced to oscillate around both gimbal axes. Hence the camera’s main axis (optical axis) describes a cone whose axis is (z).

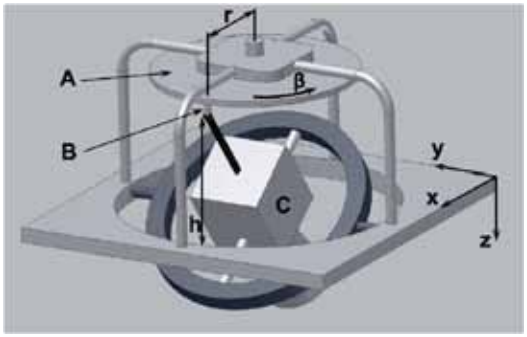

Fig. 4: Operation principle of tumbling camera.

In this way, only one control parameter (actual position of rotary element, angle β) will allow the camera to reach all four major perspectives ahead, right, back and left. In addition, arbitrary perspectives are obtainable which are circular around axis z. In remote sensing applications, the z axis points towards the nadir point. Hence the camera footprint circulates around the nadir point.

The relation between angular velocity dβ/dt and camera acquisition rate determines the overlap of two consecutive images. The direction of rotation is reversible. Velocity is adjustable from 0 deg/s up to 360 deg/s. As the rotation range is unlimited, an n × 360 deg motion is possible. The camera moves in a tumbling way, hence rotation around the optical axis is avoided, and the cabling remains torsion-free. Rotary joints are not required. Unlimited circulation plays an important role for the photogrammetric processing of images: as a result of the linear flight path the rotating oblique image footprints become a spiral, resulting in a special image block configuration. Fig. 5 shows a constellation of oblique footprints based on real data, here with an oblique angle of ~30 deg, gear steps of 45 deg and aircraft crab angle of about -10 deg. The crab-angle can be easily compensated on-the-fly by adjusting the motor's zero point position. One full circle of camera rotation is shown in blue colour. The unfilled frames show the spiral of footprints caused by flight path.

In case of an ideal flight trajectory, again by avoiding rotation about the optical axis, the yaw angle of oblique images remains unchanged. Independent of the camera orientation, each image corner remains in the same relative position, see the red marks in Fig. 5. Photogrammetric analysis can be carried out analogously to common nadir image flights using conventional algorithms. The nadir area is covered by an additional fixed camera (Fig. 6).

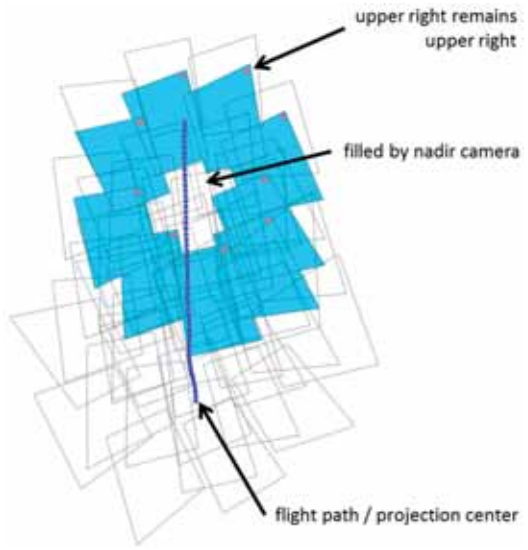

Fig. 5: Footprints characteristics of a tumbling camera. Blue dots assign the flight path. Red dots mark upper right image corners, indicating that there is no rotation about the optical axis.

3.3 *MACS-TumbleCam*

Combining nadir camera and oblique tumbling camera as shown in Fig. 6, added by peripheral devices, enables a lightweight aerial camera system for 3D data acquisition, see Fig. 7.

The oblique footprints circulate around the nadir camera's footprint. Every image has to cover a particular ground detail, not a quadrant as in penta- or triple-systems. The focal

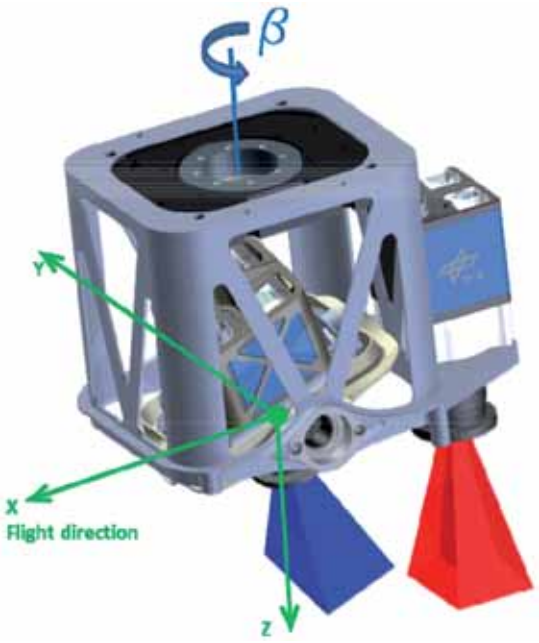

Fig. 6: Sensor head with tumbling camera (left) and a nadir camera (right); green: coordinate system of sensor head.

Fig. 7: MACS-TumbleCam.

length can be increased, resulting in higher resolution oblique images. The mounted sensors consist of two 8 megapixel industrial cameras including trigger and event interfaces. Both cameras are constructed identically and take images synchronously. A pair of images with different orientations is generated simultaneously.

With proper overlap of the oblique images the block can be oriented by AT without the use of nadir images. No AT can be processed if only a small overlap between oblique images is available, e.g. an overlap of less than about 5%, which may be caused by a fast camera rotation while using a low image acquisition rate. In this case, the following process can be used for determining the exterior orientation. One can first determine the exterior orientations of nadir images by conventional AT and then transform the exterior orientation of any nadir image to the corresponding oblique image (Wieden & Stebner 2013). As the geometric relation between both images is known, there is no need to overlap nadir and corresponding oblique image, see section 3.4.

The transformation of exterior orientation between images of any image pair is described in section 3.4. To apply this process, the correct geometric relation between both cameras needs to be known for the time of exposure. This geometric relation mainly arises from the construction of the sensor head and from the actual position of the rotary element in terms of angle β. Hence, a rigid frame for both cameras was constructed and a drive unit was assembled, see Fig. 6. The nadir camera and the drive unit are mounted stationary. By mirrored spring constraints, the gimballing of the tumbling camera is restrained from free floating that might be caused by any occurring dynamic forces. Further, any temperature-dependent shift is compensated. The weight of the rigid aluminium frame is 214 g.

The constant oblique deflection was set to an angle such that a small overlap between any oblique / nadir image pair is ensured. Thus, an associated image block is established for the images of the first camera and of the second camera, respectively. Furthermore, the images of both cameras are connected by corresponding image points. By operating these two cameras as described, an overall nadir angle combination analogous to a penta-camera head is achieved. The difference is that the tumbling camera acquires the oblique images successively and not at the same moment, as penta-camera heads do.

To move the sensor, a rotation stage of 14 mm height was integrated. It has a built-in angle encoder achieving a resolution of 34 µrad (0.002 deg). For the duration of the image acquisition the motor stops and delivers its actual angular position (angle β) to the computer. Afterwards, the motor rotates the camera to the position for the next image.

Mainly due to weight restrictions the direct georeferencing is produced by a MEMS-based GNSS-aided attitude and heading reference system (AHRS) consisting of a 6 degree of freedom IMU, 3D magnetometer and L1 C/A code GNSS receiver. The AHRS-data are UTC-time stamped with a rate of 120 Hz. Bias stability of the IMU is 1 deg/s for the gyros and 0.02 m/s^2 for the accelerometers, respectively. The noise is 0.05 deg/s/sqrt(Hz) for the gyros and 0.002 $m/s^2/sqrt(Hz)$ for the accelerometers, respectively. The built-in magnetometers as well as a GNSS solution assist the AHRS to compensate the IMU drifts and enable the output of earth-referenced Euler-angles roll, pitch and heading.

For the AT and 3D modelling, the geodetic position of the projection centres is of much higher importance. Hence, an L1/L2 GNSS receiver for post-processing raw measurements including reference stations was used. The accuracy thus obtained is evaluated in section 4. The general set-up of MACS-TumbleCam is shown in Tab. 1. As a main attribute it should

be noted that the fully operational system has a weight of less than 4 kg plus 1 kg for the payload battery. ATISS is made for a payload of up to 10 kg.

3.4. *Geometric Accuracy*

The geometric relation between nadir camera and oblique camera requires lever arms and angular offsets dependent on the rotational element position. The lever arms are determined directly from the CAD-model. Angular offsets are calculated using the equations

$$\varphi(\beta) = \sin(\beta) * \gamma \quad (1)$$

$$\theta(\beta) = \cos(\beta) * \gamma \quad (2)$$

$$\psi = 0 \quad (3)$$

where
φ (roll), θ (pitch) and ψ (yaw) = rotation angles around the sensor head coordinate frame axes x, y and z, respectively (see Fig. 6),
β = angular motor position and
γ = deflection angle of the oblique camera (30 deg, fixed).

These values are used to compute the rotation matrix which transforms the oblique camera orientation into the sensor head coordinate frame (x,y,z-coordinate frame in Fig. 6). A second rotation matrix is used to transform the sensor head coordinate frame into the terrestrial frame with the help of Euler angles, which are provided by the AHRS. Angular correction values (boresight corrections) which depend on the actuator-position have additionally been applied to the angular offsets between the camera and the sensor head frames. This is necessary as a result of manufacturing and assembly imprecision, tolerances within the kinematic chain and angular encoder uncertainty. The boresight corrections have been determined photogrammetrically using the mathematical principle of projective reconstruction. In a laboratory set-up a calibrated camera Canon EOS 5D was fixed to the sensor head frame. Its images played the role

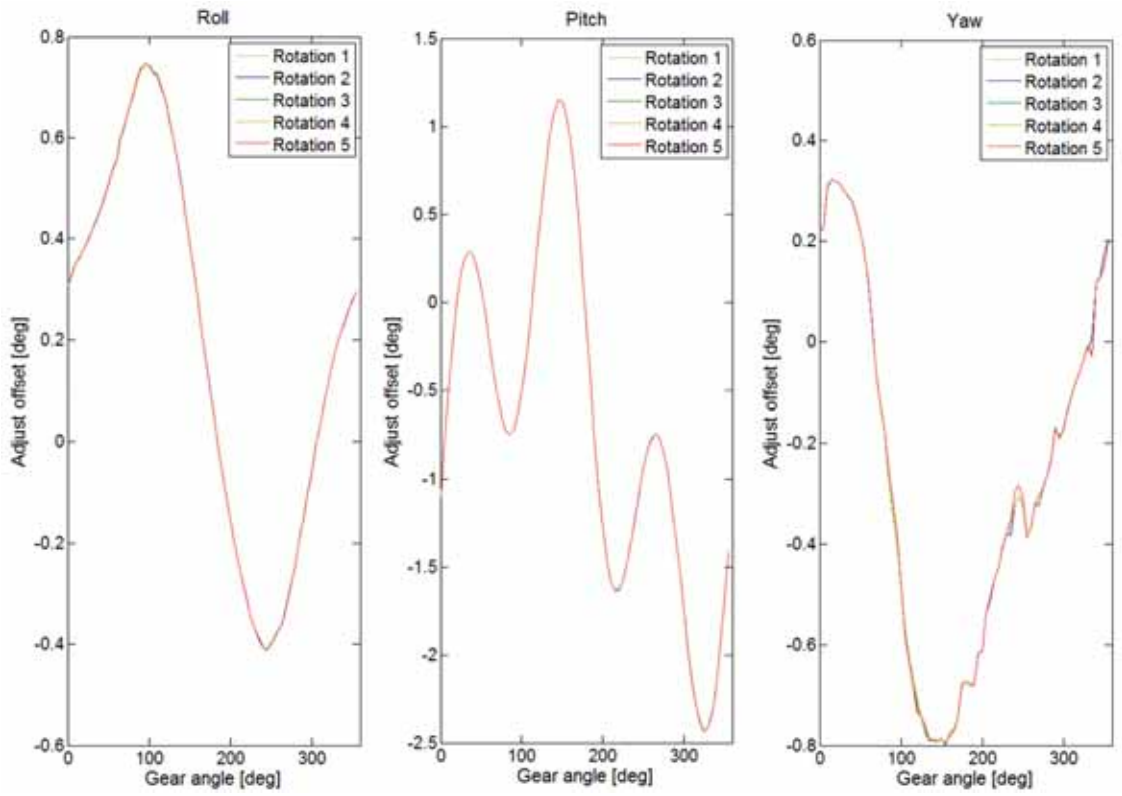

Fig. 8: Angular boresight corrections for Roll, Pitch and Yaw, repeated for 5 full circles.

of joining the minimally overlapping images of nadir and oblique cameras. The EOS 5D images remained static and covered the footprint of all possible oblique footprints. Consequently the nadir camera's footprint was covered as well. The motor turned in steps of 5 deg. At every rest position the images of all three cameras were taken simultaneously. For analyzing the repeat accuracy five full circles of the oblique rotating camera were carried out, leading to 361 image triplets. Executing block matching (MATHWORKS 2013) on each of the static camera images showed that this camera did not change orientation. Thus, just one EOS 5D image could be used as a reference. The purpose of this image was the concatenation of all oblique images. Any oblique image, the nadir image and the concatenation image are projected onto the same plane. Aided by 5323 features, for each of the oblique images the relative angular offset to the reference image was determined. Fig. 8 shows the difference between angles derived by (1) to (3) and real angles determined by the photogrammetric procedure. For each axis and every actuator position, these values are the boresight corrections.

Repeat accuracies for all the five passages are shown in Tab. 2. For the 5 boresight correction curves of roll, pitch and yaw (Fig. 8) mean value curves are calculated, respectively. The determined standard deviations are related to the mean value curves.

The standard deviations indicate that the angular error between any projected oblique image and the projected nadir image is less than 1 pixel (2σ). Hence the sensor head consisting of drive unit, gimballed mount and two cameras complies with the requirements of a photogrammetric camera system.

Fig. 9: Image mosaic generated by applying the angles φ, θ and ψ and additional boresight corrections for the oblique images.

As the correction values are very small, they are applied as additive corrections to the angular offsets, and the corrected values are used to compute the rotation matrix R which transforms the camera orientations. So the exterior orientation of the nadir camera can be converted into the exterior orientation of the oblique camera and vice versa.

To show that there is 1 pixel accuracy, the boresight corrections for one full circle of oblique images have been considered to form a stitched picture, see Fig. 9. The single images are taken from the laboratory set-up. Images of 5 deg angular position offsets are stitched without any image analysis or interpretation. A deeper analysis of the accuracies that can be achieved by the MACS-TumbleCam is given in (WIEDEN & STEBNER 2014).

Tab. 2: Repeat accuracies, 5 times any of 72 angular actuator positions.

	Mean standard deviation (2σ)	**Max standard deviation** (2σ)
Φ (roll)	8.6/1000 deg	10/1000 deg At photo 219
Θ (pitch)	7.8/1000 deg	17/1000 deg At photo 003
Ψ (yaw)	35.9/1000 deg	96/1000 deg At photo 003

4 Test Flight

In April 2012 some test flights were conducted using ATISS as carrier. Steered by the autopilot system, 10 parallel flight lines were passed, see Fig. 10. The target area was 1 × 0.3 km^2. The operating height was approximately 200 m above ground level, resulting a ground sampling distance (GSD) of approximately 3 cm at nadir.

For one flight, conventional AT was processed on 726 nadir images by using 6 ground control points (GCP). Further for the projection centres of the nadir images RTK GNSS positions and additional AHRS attitude data were introduced. The internal accuracy of the AT was determined to be 0.1 pixels. Tab. 3 shows the mean standard deviations of the projection centres.

With the help of semi-global matching (SGM) the nadir images were used to generate a digital elevation model (DEM). Afterwards, an orthomosaic was processed. Fig. 11 shows a single oblique image, one of multiple images used to texturize façades following the procedure described in section 3.4. Based on the texturized 3D-model, interactive visualizations can be established. Fig. 12 shows a screenshot of such a visualisation. Each pixel has a well-defined spatial coordinate. The virtual model is based on data exclusively derived by MACS-TumbleCam. Further processing such as the determination of roof geometries, tree counting, classifications etc. can be applied.

5 Conclusions and Future Work

A self-sustaining 3D-capable photogrammetric aerial camera system was presented which requires less than 5 kg capacity. A nadir camera was applied to determine exterior orientations and to derive outputs such as digital elevation models and orthomosaics. The single oblique camera is enabled by robotic actuation to cover perspectives around nadir. The oblique camera's rotation about the optical axis is avoided by the described tumbling movement concept. While the camera rotation is not limited, the cabling is kept free from torsion and consequently rotary joints

Tab. 3: SD of nadir images exterior orientation.

Mean SD translations (m)		**Mean SD rotations (deg)**	
X	0.012	**Omega**	3.7/1000
Y	0.013	**Phi**	3.8/1000
Z	0.021	**Kappa**	1.2/1000

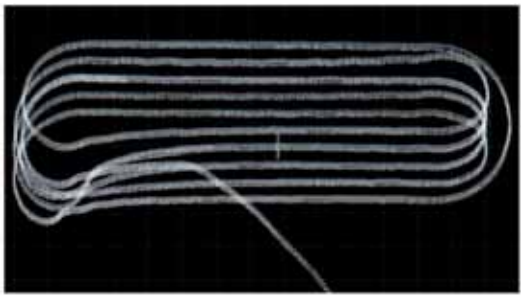

Fig. 10: ATISS test-flight path.

Fig. 11: Single raw oblique image.

Fig. 12: Screenshot of interactive 3D-visualization.

can be omitted. Further image processing is faster as there is one degree of freedom less. The system was used on the UAV ATISS for automated, high resolution and pixel-accurate façade texture without aerotriangulation of its oblique images.

In further steps on-the-fly crab angle compensation is examined, the motor assembly is intended to be significantly reduced in weight, and the actuator is to be used to establish forward motion compensation. A second unconstrained degree of freedom, introducing variable radius (r) can be implemented to make the oblique angle adjustable. Hence, all perspectives around nadir could be reached. Even nadir orientation could be set. If the movement of the camera works fast enough, the fixed nadir camera then can be rejected.

The ATISS measurement UAV is still part of the SALSA project. Further development on ATISS is to improve safety operation by integrating a parachute rescue system and a triple redundant autopilot system.

Acknowledgement

The project described in this paper was supported by the federal state Brandenburg and the European Union by the EFRE-WiTet program www.efre.brandenburg.de.
The authors of MACS-TumbleCam want to thank especially the team of Neurorobotics Research Laboratory at the Humboldt-Universität zu Berlin who manufactured the sensor head frame and the motor control unit and the whole team of DLR OS-ASK who assembled, software engineered and post-processed all data.
Thanks also to the people from "Investitionsbank des Landes Brandenburg" ILB for their support of the SALSA project.

References

Cramer, M., Haala, N., Rothermel, M., Leinss, B. & Fritsch, D., 2013: UAV-gestützte Datenerfassung für Anwendungen der Landesvermessung – das Hessigheim-Projekt. – DGPF Tagungsband **22:** 450–469.

Danders, Ch., 2007: Entwurf und Konstruktion der Flugmessdrohne ATISS. – Bachelor thesis, Technical University of Applied Sciences Wildau, 2007.

Eisenbeiss, H., 2009: UAV Photogrammetry. – Dissertation, Eidgenössische Technische Hochschule Zürich, Schweiz.

Heinze, N., Esswein, M., Krüger, W. & Saur, G., 2010: Image exploitation algorithms for reconnaissance and surveillance with UAV. – SPIE 7668, Airborne Intelligence, Surveillance, Reconnaissance (ISR) Systems and Applications VII, 76680U, April 26, 2010.

Küng, O., Strecha, C., Beyeler, A., Zufferey, J.-C., Floreano, D., Fua, P. & Gervaix, F., 2011a: The accuracy of automatic photogrammetric techniques on ultra-light uav imagery. – International Archives of the Photogrammetry, Remote Sensing and Spatial Information Sciences, ISPRS **XXXVIII-1/C22:** 125–130, Zurich, Switzerland.

Küng, O., Strecha, C., Fua, P., Gurdan, M., Achtelik, M., Doth, K.-M. & Stumpf, J., 2011b: Simplified building models extraction from ultra-light UAV imagery. – International Archives of the Photogrammetry, Remote Sensing and Spatial Information Sciences, ISPRS **XXXVIII-1/C22:** 217–222, Zurich, Switzerland.

Lehmann, F., Berger, R., Brauchle, J., Hein, D., Meissner, H., Pless, S., Strackenbrock, B. & Wieden, A., 2011: MACS – Modular Airborne Camera System for Generating Photogrammetric High-Resolution Products. – PFG – Photogrammetrie, Fernerkundung, Geoinformation **2011** (6): 435–446.

Li, Z. & Li, Y., 2011: Photogrammetric recording of ancient buildings by using unmanned helicopters – cases in China. – International Archives of the Photogrammetry, Remote Sensing and Spatial Information Sciences, ISPRS **XXXVIII-1/C22:** 189–193, Zurich, Switzerland.

Mathworks, 2013: http://www.mathworks.de/de/help/vision/ref/blockmatching.html (24.5.2013).

Meissner, H. & Pless, S., 2011: MACS –Modular airborne camera system for generating photogrammetric high-resolution products. – PFG – Photogrammetrie, Fernerkundung, Geoinformation **2011** (6): 435–446.

Neitzel, F. & Klonowski, J., 2011: Mobile 3D mapping with a low cost UAV system. – International Archives of the Photogrammetry, Remote Sensing and Spatial Information Sciences, ISPRS **XXXVIII-1/C22:** 39–44, Zurich, Switzerland.

Remondino, F., Barazzetti, L., Nex, F., Scaioni, M. & Sarazzi, D., 2011: UAV photogrammetry for mapping and 3d modelling – current status and

future perspectives. – International Archives of the Photogrammetry, Remote Sensing and Spatial Information Sciences, ISPRS **XXXVIII-1/C22:** 25–31, Zurich, Switzerland.

Seiler, I., 2013: Gemeinsame Grundsätze des Bundes und der Länder für die Erteilung der Erlaubnis zum Aufstieg von unbemannten Luftfahrtsystemen gemäß § 16 Absatz 1 Nummer 7 Luftverkehrs-Ordnung (LuftVO). – Bundesministerium für Verkehr, Bau und Stadtentwicklung, Referat LR 24, Bonn.

Wenzel, K., Rothermel, M., Fritsch, D. & Haala, N., 2013: Image acquisition and model selection for multi-view stereo. – International Archives of the Photogrammetry, Remote Sensing and Spatial Information Sciences, ISPRS **XL-5/W1:** 251–258, 3D-ARCH 2013, Trento, Italy.

Wieden, A. & Stebner, K., 2013: Referenzorientierung für Bilddaten aus Mehrkopfkamerasystemen. – DGPF Tagungsband **22:** 518–525.

Wieden, A. & Stebner, K., 2014: Accuracy Analysis for Automatic Orientation of a Tumbling Oblique Viewing Sensor System. – EuroCOW **2014:** 131–136, Barcelona, Spain.

Zhang, C. & Kovacs, J., 2012: The application of small unmanned aerial systems for precision agriculture: a review. – Precision Agriculture **13** (6): 693–712.

Addresses of the Authors:

Jörg Brauchle & Ralf Berger, DLR, German Aerospace Center, Institute of Optical Sensor Systems, 12489 Berlin, Tel: +49-30-67055-274, -572, e-mail: {joerg.brauchle}{ralf.berger}@dlr.de

Prof. Dr.-Ing. Wolfgang Rüther-Kindel, University of Applied Sciences Wildau, Department of Aeronautical Engineering, Bahnhofstraße, 15745 Wildau, Tel: +49-3375-508613, e-mail: wkindel@th-wildau.de

Manuskript eingereicht: Oktober 2013
Angenommen: Mai 2014